Time-of-Flight Positron Emission Tomography with Resistive Plate Chamber Detectors: An Unlikely but Promising Approach

Miguel Couceiro

Acta Physica Polonica Series a

Proceedings of the II Symposium on Positron Emission Tomography, Kraków, September 21–24, 2014

Time-of-Flight Positron Emission Tomography with Resistive Plate Chamber Detectors: An Unlikely but Promising Approach

M. Couceiro[a,b,*], P. Crespo[a,c], A. Blanco[a], N.C. Ferreira[d,e], L. Mendes[d,e], R. Ferreira Marques[a,c] and P. Fonte[a,b]

[a]Laboratório de Instrumentação e Física Experimental de Partículas, Departamento de Física, Universidade de Coimbra, Rua Larga, 3004-516 Coimbra, Portugal

[b]Instituto Politécnico de Coimbra, ISEC, Rua Pedro Nunes, Quinta da Nora, 3030-199 Coimbra, Portugal

[c]Departamento de Física, Faculdade de Ciências e Tecnologia, Universidade de Coimbra, Rua Larga, 3004-516 Coimbra, Portugal

[d]Instituto Biomédico de Investigação da Luz e Imagem, Faculdade de Medicina, Universidade de Coimbra, Azinhaga Santa Comba, Celas, 3004-516 Coimbra, Portugal

[e]Instituto de Ciências Nucleares Aplicadas à Saúde, Faculdade de Medicina, Universidade de Coimbra, Azinhaga Santa Comba, Celas, 3004-516 Coimbra, Portugal

The cost-effectiveness of resistive plate chamber detectors and their very good timing characteristics, open the possibility to build affordable time-of-flight positron emission tomography systems with a large axial field-of-view. Simulations suggest that, under reasonable assumptions, the absolute 3D true sensitivity, spatial resolution, and noise equivalent count rate of such systems for human whole-body screening, may exceed that of present crystal-based PET technology. However, due to the lack of energy resolution, although having energy sensitivity, the scatter fraction is expected to be considerably higher than that presented by crystal-based PET scanners. In the present paper, the simulation work done so far to access the expected performance of a resistive plate chamber time-of-flight-PET system with 2400 mm length axial field-of-view, a time resolution of 300 ps full width at half maximum for photons pairs, and depth-of-interaction information, will be revised.

DOI: 10.12693/APhysPolA.127.1453

PACS: 87.57.uk, 29.40.Cs, 87.57.cf, 87.57.cm

1. Introduction

The resistive plate chamber (RPC) time-of-flight (TOF) positron emission tomography (PET) concept [1] is based on the converter plate principle [2], depicted in Fig. 1.

Simple and economic construction, even for large area covering, good timing resolution of 300 ps full width at half maximum (FWHM) for 511 keV photon pairs [1], excellent position accuracy of 38 μm [3], and the capability to resolve the depth-of-interaction (DOI) [1], make RPC detectors an alternative for developing PET scanners with a large axial field-of-view (AFOV) almost free of parallax errors and with TOF capability. As the major disadvantage when compared to inorganic crystal scintillation detectors, one can point out the lack of energy resolution. However, for the detection of photons, RPCs present an energy sensitivity [5, 6], which, for PET applications, is equivalent to an energy discrimination threshold of 300 keV in terms of rejection of coincidences involving scattered photons [1].

*corresponding author; e-mail: couceiro@coimbra.lip.pt

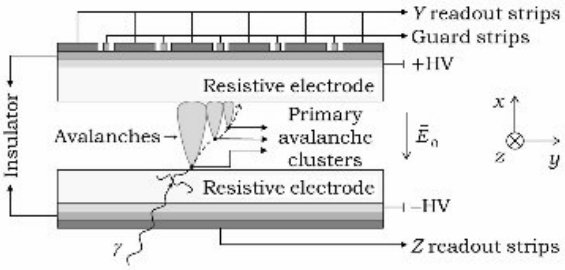

Fig. 1. Scheme of a single gap timing RPC detector with position readout, depicting the converter plate principle.

In the present paper, the simulation work done so far to access the expected performance of a full-body length RPC TOF-PET scanner, will be briefly revised. Full description of (and details on) the simulation work done so far can be found in Refs. [6–41].

2. Simulation setup and procedures

To access the expected performance of a large AFOV RPC TOF-PET scanner, in what concerns the sensitivity, spatial resolution (SR), scatter fraction (SF), count rates (CR), and noise equivalent count rate (NECR),

as measured by the National Electrical Manufacturers Association (NEMA) NU2 standards [12, 13], simulations were performed with programs developed with the GEANT4 toolkit [14, 15]. For the sensitivity test, the 1994 and the 2001 versions of the NEMA NU2 standards [12, 13] were used, while for the SR, SF and NECR tests, only the NEMA NU2-2001 standards [13] were employed.

In what follows, the general setup employed for the simulations concerning each of the aforementioned performance parameters will be given shortly.

2.1. Sensitivity

For the sensitivity test following the NEMA NU2-1994 standards [12], the scanner was modelled as a right circular annulus with 927 mm inner diameter and an AFOV ranging from 150 mm to 2400 mm [6, 7]. The test phantom consisted in a 1750 mm axially extended version [6, 7] of the phantom defined in the NEMA NU2-1994 standards [12]: a 3 ± 1 mm thick right circular cylindrical polymethyl methacrylate (PMMA) shell, with an outer diameter of 203 ± 3 mm and an inner axial length of 190 ± 1 mm, with the core filled with a given activity diluted in water. The physics list employed was entirely based on the standard electromagnetic physics (SEP) models of the GEANT4 toolkit [14, 15], and the source was defined as positrons at rest, uniformly distributed in the core of the test phantom [6, 7].

For the sensitivity test following the NEMA NU2-2001 standards [13], the scanner was defined in a approxilar way, but with a diameter of 920 mm and a fixed AFOV of 2400 mm [9], and the test phantom consisted in that defined in the NEMA NU2-2001 standards [13]: a line source with an axial length of 700 mm, which is surrounded by a variable thickness of aluminium by means of five concentric 2.5 mm thick cylindrical sleeves that are added in turn around the line source. An axially extended version of the phantom, with a length of 2400 mm, was also simulated [9]. The physics list employed was based on the low energy electromagnetic package (LEP) of the GEANT4 toolkit [14, 15], and the source consisted in back to back photons uniformly distributed in the core of the line source [9].

In both cases, the phantoms were centred in the scanner field-of-view (FOV), photons were fully tracked in the phantom, and the points were the photons impinged the inner surface of the detection annulus were taken as the detection points [6, 7, 9].

2.2. Scatter fraction, count rates and noise equivalent count rate

For the SF, CR, and NECR tests, the scanner was defined as depicted in Fig. 2: a hollow parallelepiped with four detections heads, each containing a stack of twenty double-module multi-gap RPCs, each module having six 200 μm thick glass plates separated by five 350 μm thick amplification gaps, each module having its own axial readout electrode, the transaxial electrode being shared by both modules [10, 11].

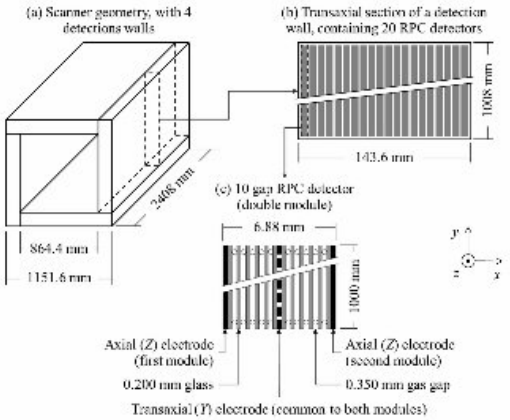

Fig. 2. Sketch of the RPC TOF-PET system [10, 11]: (a) scanner, consisting of 4 detection walls; (b) detection wall containing a stack of 20 double module multi gap RPC detectors; (c) RPC detector with two detection modules, each containing 6 glass plates with thicknesses of 200 μm, separated by 5 amplification gaps with individual thicknesses of 350 μm, with a common transaxial and two independent axial readout electrodes.

The test phantom, which was centred in the FOV, consisted in that defined in the NEMA NU2-2001 standards [13]: a right circular cylinder of polyethylene with specific gravity of 0.96 ± 0.01, an axial length of 700 ± 5 mm, and a diameter of 203 ± 3 mm, in which a hole with 6.4 ± 0.2 mm diameter is drilled parallel to the central axis of the phantom but displaced 45 ± 1 mm from it, which serves to accommodate a line source consisting in a right circular cylindrical annulus (also of polyethylene) with inside and outside diameters of, respectively, 3.2 ± 0.2 mm and 4.8 ± 0.2 mm, the core being filled with a given activity diluted in water. An axially extended version of the phantom, with an axial length of 1800 mm, was also simulated [10, 11]. For both phantoms, the source consisted in ^{18}F nuclei uniformly distributed in the core of the line source [10, 11].

The physics list employed was based on the SEP models of the GEANT4 toolkit [14, 15], except for [10, 11]: (1) the Rayleigh interaction, for which the LEP provided by the GEANT4 toolkit [14, 15] was used, and (2) the positron annihilation physics, for which the routine provided by GATE [16], accounting for the photon acollinearity [16], was implemented in the physics list of the programs developed with the GEANT4 toolkit [14, 15]. Photons were fully tracked in the phantom and in the scanner, and electrons were fully tracked if generated inside a glass plate, the track being killed if they reached an amplification gap [10, 11].

2.3. Spatial resolution

For the SR test, the scanner was defined as mentioned in Sect. 2.2, except for the detectors, which were set to 40 single-module multi-gap RPC detectors, approxilar to those presented in Fig. 2, each having its own transaxial

and axial readout electrodes [8, 11]. The phantom consisted in a spherical point-like water core with 1 μm diameter enclosed in a 2 mm outer diameter shell of PMMA, placed in the scanner center and in the central transaxial plane but displaced 100 mm in both the scanner X and Y directions [8, 11]. The physics list employed in the SR test, was approxilar to that employed in the SF, CR and NECR tests, and the particle tracking was performed in the same way [8, 11]. The source consisted of positrons at rest uniformly distributed in the phantom core [8, 11].

3. Simulation data processing

The processing of simulation produced data was performed in cascade stages by programs developed externally to the programs developed with the GEANT4 toolkit [14, 15]. In what follows, those stages will be addressed.

3.1. Decay times

For all tests, decay times randomly drawn from an exponential distribution with a given activity and the ^{18}F decay constant (and β^+ branching ratio, if the source consisted in positrons at rest or in back-to-back photons), were assigned to the photon flight times of single hits, which were then affected by a 90 psσ Gaussian time jitter to account for the 300 ps FWHM TOF resolution [6–11].

The activity considered for the sensitivity tests (both with the 1994 and the 2001 versions of NEMA NU2 standards [12, 13]), was set to a value low enough so that losses due to detector dead time and random coincidences were negligible [6, 7, 9, 11]. For the SR test, an activity of 370 kBq (10 μCi) was used [8, 11]. The activity considered for the SF test was of 37 kBq (1 μCi), and for the CR and NECR tests, activities ranging from 37 kBq (1 μCi) to 370 MBq (10 mCi) were used [10, 11].

3.2. Detection efficiency

For the sensitivity test, the detection efficiency was modelled according to the curves presented in Fig. 3, obtained by simulating (with the GEANT4 toolkit [14, 15]) the extraction efficiencies of stacks of 61 and 121 glass plates with individual thicknesses of 0.4 mm, separated by, respectively, 60 and 120 amplification gaps with individual thicknesses of 350 μm [6, 9, 11].

For the SR, SF, CR, and NECR tests, photons were fully tracked in the scanner, the detection efficiency being then accounted for in the simulation.

3.3. Detector readout

For the sensitivity tests, the detection points were binned according to the segmentation of the General Electric (GE) Advance scanner, and the detector readout was not accounted for [6, 7, 9, 11].

For the SR, SF, CR, and NECR tests, the detection points of single events were considered to be those on the opposite side of the amplification gap relative to the extraction point, computed along the electron momentum direction [8, 10, 11]. The resulting detection points were

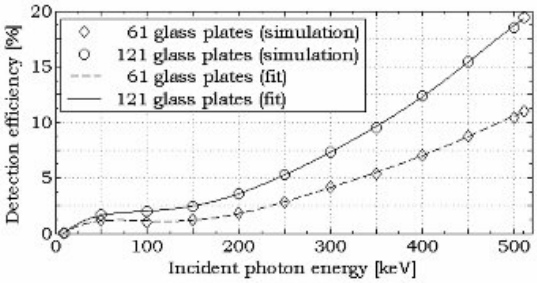

Fig. 3. Detection efficiency of stacks of 61 and 121 glass plates with individual thicknesses of 400 μm (defining, respectively, 60 and 120 amplification gaps with individual thicknesses of 350 μm), as a function of the incident photon energy, for photons impinging the first glass perpendicularly to its surface [6, 9, 11].

then processed to account for the segmentation of the detector as described in Refs. [8, 10, 11], the final detection point being then binned to 2 mm along the axial and transaxial directions (corresponding to the current pitch of the pickup strips), and to the middle of the detection module, in bins of 3.44 mm (the thickness of each detection module), leading to a maximum DOI error (along the radial direction) of 1.72 mm (half the module thickness) [8, 10, 11]. For the SR test, bins of 1 mm along the transaxial and axial directions, and continuous detection along all directions (transaxial, axial, and radial), were also considered [8, 11].

3.4. Coincidence processing

Single events resulting from the processing stage to account for the detector readout, were then fed to a coincidence sorter. For the sensitivity test, a 12.5 ns single time window (STW) coincidence sorter (for which, at a given time, only one coincidence time window, opened by the triggering event, is active), was used, and multiple coincidences were discarded [6, 7, 9, 11]. For the SR test, a STW coincidence sorter was also used, but with a 4 ns time window, and multiple coincidences were also discarded [8, 11].

For the SF, CR and NECR tests, 5 ns STW and multiple time window (MTW) coincidence sorters (for which, each event opens its own coincidence time window) were considered, and all possible coincidence pairs (including all those that can be formed from the multiple coincidences) were then processed to account for the performance test [10, 11]. (For a complete discussion concerning the use of all possible coincidence pairs, refer to Refs. [10, 11].)

3.5. Geometric acceptance of lines of response

For the sensitivity test, all coincidences defining lines of response (LORs) that traversed the scanner bore, were retained [6, 7, 9, 11], while for the SR test, only those LORs that traversed the scanner bore with a polar acceptance angle less than or equal to 9° were considered [8, 11].